



Title	Synthesis and Characterization of an Air-Stable Tin(IV) $\beta$ -Tetracyanoisophlorin Complex: Enhanced Antiaromaticity through Metal Complexation.
Author(s)	Sugimura, Haruna; Nakajima, Kana; Yamashita, Ken-ichi
Citation	Asian Journal of Organic Chemistry. 2025, p. e202400550
Version Type	VoR
URL	<a href="https://hdl.handle.net/11094/100185">https://hdl.handle.net/11094/100185</a>
rights	This article is licensed under a Creative Commons Attribution-NonCommercial 4.0 International License.
Note	

*The University of Osaka Institutional Knowledge Archive : OUKA*

<https://ir.library.osaka-u.ac.jp/>

The University of Osaka

# Synthesis and Characterization of an Air-Stable Tin(IV) $\beta$ -Tetracyanoisophlorin Complex: Enhanced Antiaromaticity through Metal Complexation

Haruna Sugimura,<sup>[a]</sup> Kana Nakajima,<sup>[a]</sup> and Ken-ichi Yamashita<sup>\*[a, b]</sup>

Isophlorins, which are two-electron reduced porphyrins, have garnered significant interest because of their potential antiaromaticity and unique electronic properties. However, the isolation of stable antiaromatic isophlorins remains challenging because they are prone to oxidation or reduction to the corresponding aromatic molecules, or are structurally distorted, resulting in loss of antiaromaticity. Here, we report the synthesis and characterization of a Sn(IV)  $\beta$ -tetracyanoisophlorin complex obtained through two-electron reduction of the corresponding Sn(IV)  $\beta$ -tetracyanoporphyrin complex. This Sn(IV) complex exhibits enhanced antiaromaticity owing to its highly planar structure, facilitated by the central Sn atom. X-ray crystal

diffraction analysis revealed that the Sn(IV) isophlorin complex contains two methoxy groups as axial ligands and that it exists as a divalent anion, demonstrating the oxophilic nature of the Sn(IV) isophlorin complexes. Notably, this Sn(IV) isophlorin complex is stable under air, distinguishing it from previously reported Si(IV) and Ge(IV) isophlorin complexes without cyano groups. This study thus presents the first isolation of an air-stable metal complex of antiaromatic isophlorin, opening new possibilities for exploring the unique properties of antiaromatic porphyrinoids for various applications, including catalysis and materials science.

## Introduction

Isophlorins, which are the two-electron-reduced forms of porphyrins, were first proposed by Woodward as intermediates in porphyrin synthesis.<sup>[1-3]</sup> According to Hückel's theory, these compounds potentially possess  $20\pi$  antiaromatic character. Antiaromatic molecules, including isophlorins, are typically unstable, prone to oxidation or reduction to the corresponding aromatic molecules, or are structurally distorted, resulting in loss of antiaromaticity. Isophlorins tend to become nonaromatic because of the disrupted planarity caused by steric hindrance from the hydrogen atoms at the ring center.

Two main strategies have been employed to synthesize planar and antiaromatic isophlorins: (1) introducing a bridging structure at the isophlorin center (Figure 1a) using tetravalent metals, such as Si or Ge, or their analogs, such as C=C or B-B, to enhance planarity,<sup>[4-7]</sup> and (2) replacing nitrogen atoms with heteroatoms to reduce the steric hindrance caused by the inner

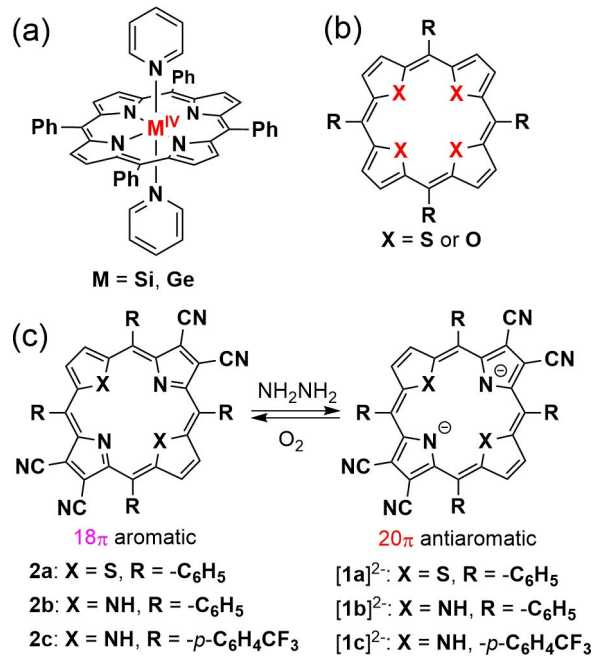


Figure 1. Reported antiaromatic isophlorins that have been characterized and/or isolated.

[a] H. Sugimura, K. Nakajima, K.-i. Yamashita

Department of Chemistry, Graduate School of Science, Osaka University, 1-1 Machikaneyama, Toyonaka, Osaka 560-0043, Japan  
E-mail: yamashita-k@chem.sci.osaka-u.ac.jp

[b] K.-i. Yamashita

Innovative Catalysis Science Division, Institute for Open and Transdisciplinary Research Initiatives (ICS-OTRI), Osaka University, Suita, Osaka 565-0871, Japan

Supporting information for this article is available on the WWW under <https://doi.org/10.1002/ajoc.202400550>

© 2024 The Authors. Asian Journal of Organic Chemistry published by Wiley-VCH GmbH. This is an open access article under the terms of the Creative Commons Attribution Non-Commercial License, which permits use, distribution and reproduction in any medium, provided the original work is properly cited and is not used for commercial purposes.

NHs (Figure 1b).<sup>[8-11]</sup> Various antiaromatic isophlorins have been synthesized using these techniques.

We have previously reported the generation of antiaromatic  $\beta$ -tetracyanoisophlorins through two-electron reduction of  $\beta$ -tetracyanoporphyrins (Figure 1c).<sup>[12,13]</sup>  $\beta$ -Tetracyanoporphyrins exhibit high reduction potentials due to their four cyano groups, allowing for easy reduction by weak reducing agents such as hydrazine. The dithia analog of  $\beta$ -tetracyanoporphyrin,

**2a**, had a sufficiently high reduction potential to form the corresponding  $\beta$ -tetracyanoisophlorin [**1a**]<sup>2–</sup>.<sup>[12]</sup> However, the  $\beta$ -tetracyanoporphyrin **2b** could not be fully reduced under the conditions used to access [**1a**]<sup>2–</sup>. By introducing additional electron-withdrawing  $\text{CF}_3$  substituents on the phenyl groups, we synthesized a new  $\beta$ -tetracyanoporphyrin **2c** that could be reduced to isophlorin [**1c**]<sup>2–</sup> using hydrazine.<sup>[13]</sup> UV-Vis/NIR absorption, NMR, and crystallographic analyses confirmed the antiaromatic nature of the isophlorins.

Isophlorin–metal complexes have been studied electrochemically, including measurements on the Zn complex of *meso*-tetrarylporphyrin by Müllen et al. in 1989.<sup>[14]</sup> However, only Si(IV) and Ge(IV) isophlorin complexes have been successfully isolated.<sup>[4,5]</sup> These complexes are highly sensitive to air and challenging to handle under atmospheric conditions.

Although Group 14 elements can adopt both divalent and tetravalent oxidation states, the stability of the tetravalent state decreases in the order Si > Ge > Sn. For Sn, the inert pair effect stabilizes the divalent state more significantly than for Si or Ge.<sup>[4,5]</sup> Consequently, when  $\text{Sn}^{\text{IV}}(\text{tpp})$  ( $\text{tpp}$ =tetraphenylporphyrinato dianion) is reduced, metal reduction is favored over porphyrin reduction, which has previously prevented the isolation of Sn isophlorin complexes.<sup>[5]</sup>

$\text{Sn}(\text{IV})$ –porphyrin complexes have been studied extensively, particularly in photocatalysis and photodynamic therapy.<sup>[15,16]</sup> They are significantly easier to synthesize than other Group 14 metal–porphyrin complexes (Si(IV) and Ge(IV)) and exhibit higher reduction potentials than many other metal–porphyrin complexes.<sup>[17]</sup>

We hypothesized that using the  $\beta$ -tetracyanoporphyrin as a ligand for Sn, which has a significantly higher reduction potential than TPP, might lead to selective ligand reduction and the formation of the desired isophlorin. While  $\beta$ -tetracyanoporphyrin complexes with various metals (Zn, V, Fe, Co, Ni and Cu) have been reported in the literature,<sup>[18–25]</sup> tin complexes have yet to be synthesized. Herein, we report the synthesis of a Sn(IV) complex of  $\beta$ -tetracyanoisophlorin  $\text{SnL}_2\text{-1b}$  (L: axial ligand) (Figure 2) by reducing the corresponding Sn(IV) porphyrin  $\text{SnCl}_2\text{-2b}$ . The complex exhibits unique aromaticity/antiaromaticity properties that may lead to the development of new molecular switches or sensors.

## Results and Discussion

$\text{Sn}(\text{IV})$   $\beta$ -tetracyanoporphyrin complex  $\text{SnCl}_2\text{-2b}$  was synthesized using  $\text{SnCl}_2\text{·}2\text{H}_2\text{O}$  as reported previously.<sup>[26]</sup> The structure of  $\text{SnCl}_2\text{-2b}$  was confirmed by X-ray crystal structure, NMR, ESI-

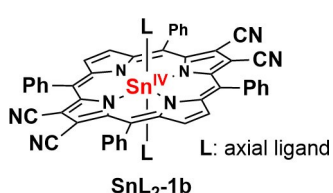


Figure 2. The target molecule in this study.

HRMS, and elemental analyses. The X-ray crystal structure (Figure 3) confirmed that  $\text{SnCl}_2\text{-2b}$  has two Cl axial ligands, indicating the complexation of a tetravalent Sn ion. The porphyrin macrocycle shows high planarity with a small mean plane deviation of 0.035 Å, similar to the reported Sn(IV) porphyrins.<sup>[15]</sup> The bond length between Cl and the Sn(IV) ion (2.4083(9) Å) was shorter than those in  $[\text{Sn}^{\text{IV}}(\text{tpp})\text{Cl}_2]$  (2.420(1) Å)<sup>[27]</sup> and  $[\text{Sn}^{\text{IV}}(\text{oep})\text{Cl}_2]$  (oep=octaethylporphyrinato dianion) (2.453(2) Å).<sup>[28]</sup> The Sn–N bond length to the five-membered ring bearing the CN groups was 2.112(3) Å and that toward the unsubstituted ring was 2.097(3) Å. These structural features are attributed to the strong electron-withdrawing properties of the cyano groups on the porphyrin periphery.

In the  $^1\text{H}$  NMR spectrum of  $\text{SnCl}_2\text{-2b}$  in  $\text{CDCl}_3$  (Figure 4a), the signal for the  $\beta$ -proton was observed at 9.1 ppm as a singlet with small satellite peaks derived from the spin–spin couplings of  $^{119}\text{Sn}$  and  $^{117}\text{Sn}$ . The coupling constant  $^4J_{\text{H-Sn}}$  was 15.2 Hz, which is in good agreement with that of  $[\text{Sn}^{\text{IV}}(\text{tpp})\text{Cl}_2]$ .<sup>[29]</sup>

The redox potentials of  $\text{SnCl}_2\text{-2b}$  were determined using cyclic and differential pulse voltammetry (Figure S2 in the Supporting Information and Table 1). In  $\text{CH}_2\text{Cl}_2$ ,  $\text{SnCl}_2\text{-2b}$  exhibited two reversible reduction waves at  $-0.42$  V and  $-0.87$  V, and an irreversible oxidation wave at  $1.42$  V. In DMSO, the reduction waves were positively shifted by approximately 0.2 V, indicating that  $\text{SnCl}_2\text{-2b}$  was more easily reduced in polar

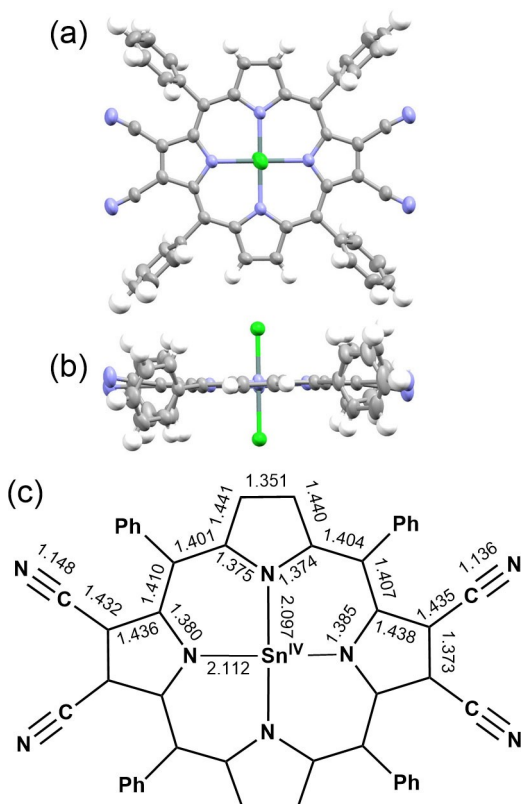
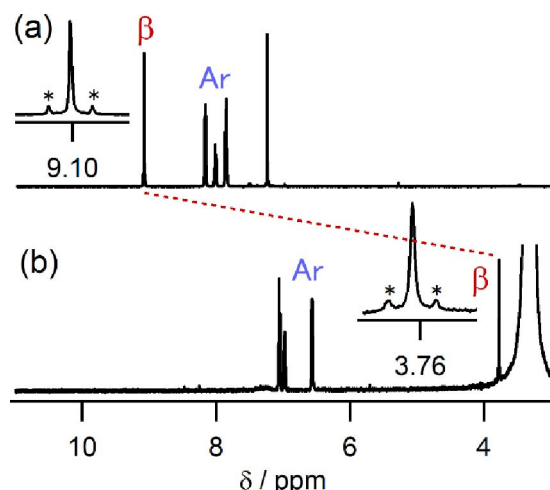


Figure 3. X-ray crystal structure of  $\text{SnCl}_2\text{-2b}$  with thermal ellipsoid representations (50% probability level). Solvated molecules (cyclohexane) are omitted for clarity. C=gray, H=white, Sn=dark blue, and Cl=green. (a) Top view, (b) side view, and (c) selected bond lengths (Å) from the crystal structure.



**Figure 4.** <sup>1</sup>H NMR spectra (500 MHz) showing the reduction of SnCl<sub>2</sub>-2b to SnL<sub>2</sub>-1b. (a) SnCl<sub>2</sub>-2b in CDCl<sub>3</sub> at 25 °C. (b) SnL<sub>2</sub>-1b was generated in situ by reduction with NH<sub>2</sub>NH<sub>2</sub>·H<sub>2</sub>O (1 drop) in [D<sub>6</sub>]DMSO at 40 °C. Asterisks indicate Sn satellite peaks.

**Table 1.** Half-wave potentials (V vs. Fc/Fc<sup>+</sup>) of SnCl<sub>2</sub>-2b, 2a, 2b, and 2c obtained from differential pulse voltammetry (DPV).

	Solvent	Eox1	Ered1	Ered2	Ered3
SnCl <sub>2</sub> -2b	CH <sub>2</sub> Cl <sub>2</sub>	(1.42) <sup>[c]</sup>	−0.42	−0.87	(−1.56) <sup>[c]</sup>
	DMSO	— <sup>[d]</sup>	−0.19	−0.60	— <sup>[d]</sup>
2a <sup>[a]</sup>	CH <sub>2</sub> Cl <sub>2</sub>	1.08	−0.54	−0.81	— <sup>[d]</sup>
	DMSO	— <sup>[d]</sup>	−0.33	−0.61	−2.19
2b <sup>[b]</sup>	CH <sub>2</sub> Cl <sub>2</sub>	(0.92) <sup>[c]</sup>	−0.75	−1.05	(−2.50) <sup>[c]</sup>
2c <sup>[b]</sup>	CH <sub>2</sub> Cl <sub>2</sub>	1.10	−0.60	−0.94	(−2.63) <sup>[c]</sup>
	DMSO	— <sup>[d]</sup>	−0.47	−0.74	(−2.42) <sup>[c]</sup>

[a] Data from ref. [12]. [b] Data from ref. [13]. [c] Irreversible peak. [d] Out of the potential range.

solvents, similar to free bases 2a, 2b, and 2c.<sup>[12,13]</sup> The second reduction potential of SnCl<sub>2</sub>-2b (−0.60 V in DMSO) was more positively shifted than 2c (−0.74 V in DMSO) and comparable to that of 2a (−0.61 V in DMSO). The difference between the second and first reduction potentials of SnCl<sub>2</sub>-2b was 0.45 V in CH<sub>2</sub>Cl<sub>2</sub> and 0.41 V in DMSO. These differences are larger than those of free bases 2a, 2b, and 2c, indicating the greater stability of the one-electron reduced form of SnCl<sub>2</sub>-2b.

The solvent had a pronounced influence on the UV-Vis/near-infrared (NIR) absorption spectra. In the UV-Vis/NIR absorption spectrum of SnCl<sub>2</sub>-2b in CH<sub>2</sub>Cl<sub>2</sub>, the Soret band was observed at approximately 450 nm, and the Q bands were observed at 600–660 nm (Figure 5), which are typical of aromatic porphyrins. In contrast, the UV-Vis/NIR absorption spectrum of SnCl<sub>2</sub>-2b in DMSO exhibited a new broad absorption band at 800–1000 nm. This behavior was also observed for free bases 2a and 2c,<sup>[12,13]</sup> and the broad bands can be attributed to the one-electron reduced anion radical of SnCl<sub>2</sub>-2b. The generation of anion radical species was also supported by electron spin resonance (ESR) measurements. The ESR spectrum of SnCl<sub>2</sub>-2b in DMSO showed a signal at *g* =

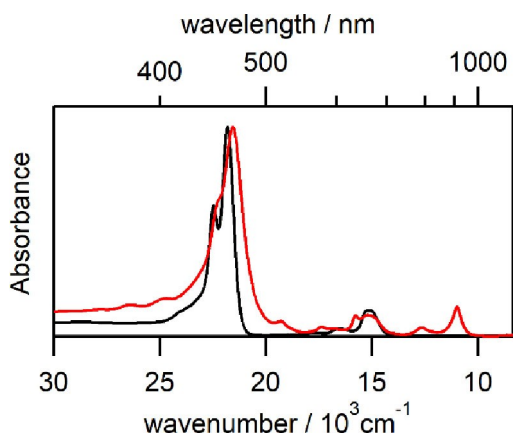


**Figure 5.** UV-Vis/NIR absorption spectra of SnCl<sub>2</sub>-2b in CH<sub>2</sub>Cl<sub>2</sub> (black) and in DMSO (red).

2.00191, supporting the generation of an anion radical (Figure S3). In contrast, no ESR signal was observed for ligand 2b in DMSO. These results are due to the higher first reduction potential of SnCl<sub>2</sub>-2b than of 2b.

The reduction of SnCl<sub>2</sub>-2b was performed as described for the reduction of 2a and 2c to obtain the corresponding isophlorin.<sup>[12,13]</sup> Treatment of SnCl<sub>2</sub>-2b with hydrazine monohydrate in DMSO resulted in a rapid color change from yellow to reddish-purple. The <sup>1</sup>H NMR spectrum of SnCl<sub>2</sub>-2b reduced with NH<sub>2</sub>NH<sub>2</sub>·H<sub>2</sub>O in [D<sub>6</sub>]DMSO indicated the formation of antiaromatic isophlorin SnL<sub>2</sub>-1b as the sole product (Figure 4b). A signal for the β-protons was observed at δ = 3.8 ppm as a singlet with Sn satellite peaks (<sup>4</sup>J<sub>H-Sn</sub> = 14.5 Hz), which was significantly upfield shifted compared to that of SnCl<sub>2</sub>-2b, suggesting a switch from an aromatic to an antiaromatic environment. The chemical shift was more upfield shifted compared to the reported free bases [1a]<sup>2-</sup>, [1b]<sup>2-</sup>, and [1c]<sup>2-</sup> (5.0–5.2 ppm),<sup>[12,13]</sup> which indicated that the complexation of the Sn(IV) ion enhanced the antiaromaticity in SnL<sub>2</sub>-1b. However, compared to the corresponding chemical shifts of previously reported Ge(IV)<sup>[5]</sup> and Si(IV)<sup>[4]</sup> isophlorins without cyano groups (0.6 and 1.3 ppm, respectively), this chemical shift was more downfield shifted. This suggests that the antiaromaticity of SnL<sub>2</sub>-1b is weaker than that of those Ge and Si isophlorins. This difference is likely not due to the change in metal, but rather, as we have previously discussed,<sup>[12,13]</sup> the electronic perturbation of the isophlorin macrocycle by π-conjugation with the cyano groups, which reduces the antiaromaticity. The obtained isophlorin SnL<sub>2</sub>-1b was stable in the presence of hydrazine even under the air like [1a]<sup>2-</sup> and [1c]<sup>2-</sup>.

From the NMR analyses, we could not determine the axial ligands L of SnL<sub>2</sub>-1b in solution; possible candidates are solvated molecules (DMSO, H<sub>2</sub>O, and NH<sub>2</sub>NH<sub>2</sub>) and OH or Cl anions. Therefore, ESI-MS measurements were performed to determine the axial ligands. Because DMSO is generally unsuitable as a solvent for ESI-MS measurements, we prepared samples by diluting the DMSO solution of SnL<sub>2</sub>-1b with a large excess of methanol prior to measurement. The primary ion peaks observed in the resulting spectrum were attributed to

species in which the axial ligands had been substituted with methoxy groups, i.e.  $[\text{Sn}(\text{OMe})_2\text{-1 b}]^{2-}$  (Figure S4). This substitution is likely due to the high affinity of Sn ions for oxygen-based anions.<sup>[30]</sup> Notably, we were not able to detect clear ion peaks for samples in the other solvents.

This ligand exchange was also observed in the X-ray crystal diffraction analysis. The single crystals were only obtained by slow diffusion of tetraphenylphosphonium bromide in methanol into a solution of **SnCl<sub>2</sub>·2b** that had been reduced with NH<sub>2</sub>NH<sub>2</sub>·H<sub>2</sub>O in DMSO. The X-ray crystal diffraction analysis revealed the molecular structure of [Sn(OMe)<sub>2</sub>·1b](PPh<sub>4</sub>)<sub>2</sub> (Figure 6). In the crystal structure, isophlorin had two methoxy ions as the axial ligands and two PPh<sub>4</sub><sup>+</sup> ions were incorporated into the crystal for each molecule, indicating tetravalent Sn ions. The isophlorin macrocycle had high planarity with a small mean plane deviation value of 0.053 Å. This high planarity contrasts sharply with the significant distortion observed in previously reported Ge(IV) and Si(IV) isophlorins without cyano groups.<sup>[4,5]</sup> This difference can be attributed to the Sn(IV) ion having an

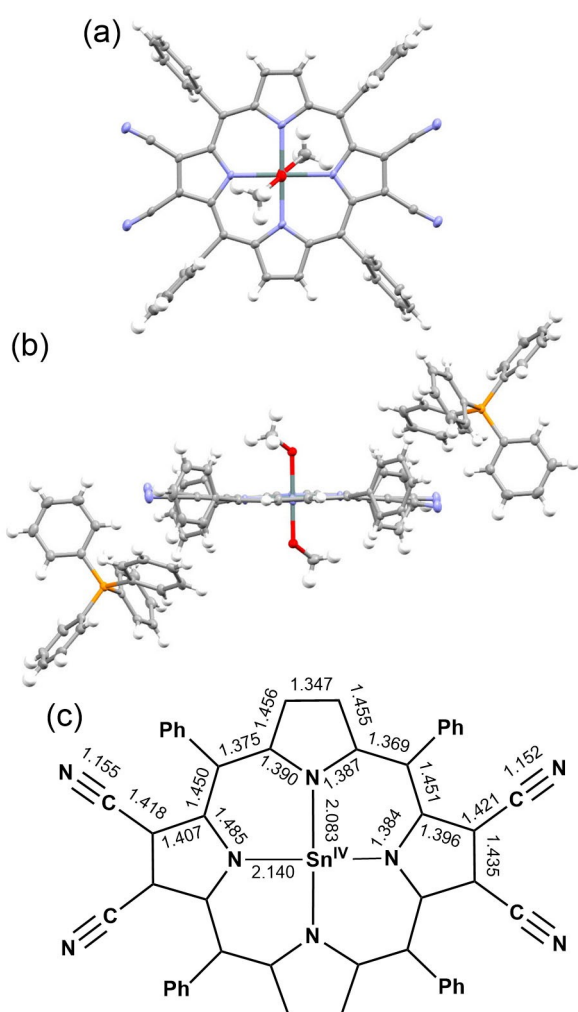


**Figure 6.** X-ray crystal structure of  $[\text{Sn}(\text{OMe})_2 \cdot \mathbf{1b}]^{2-}$  with thermal ellipsoid representations (50 % probability level). Solvation molecules (methanol) are omitted for clarity. C = gray, H = white, N = blue, Sn = dark blue, O = red, and P = orange. (a) Top view without the  $\text{PPh}_4^+$  cations, (b) side view with the  $\text{PPh}_4^+$  cations, and (c) selected bond lengths (Å) from the crystal structure.

ideal ionic radius for fitting inside the porphyrin ring, as well as the weaker antiaromaticity of **SnL<sub>2</sub>-1b** compared to the reported Ge(IV) and Si(IV) isophlorins. A more significant bond length alternation was observed compared to that of the porphyrin **SnCl<sub>2</sub>-2b** (Figure 3), which suggests a loss of aromaticity in **[Sn(OMe)<sub>2</sub>-1b](PPh<sub>4</sub>)<sub>2</sub>**.

The Sn–N bond lengths of 2.140(1) and 2.083(1) Å were comparable to those of **SnCl<sub>2</sub>–2b**. These bond lengths together with the octahedral six-coordinate geometry around the Sn ion, clearly indicates the Sn(IV) oxidation state, as a Sn(II) complex would exhibit elongated bond lengths and prefer a four-coordinate geometry.<sup>[15,31]</sup>

The nucleus-independent chemical shift (NICS) of  $[\text{Sn}(\text{OMe})_2\text{-1 b}]^{2-}$  also confirmed its antiaromatic character. The NICS values of  $[\text{Sn}(\text{OMe})_2\text{-1 b}]^{2-}$  and previously reported  $[\text{1 b}]^{2-}$  are listed in Table 2. The positive NICS(0) value of 9 at point *a* of  $[\text{Sn}(\text{OMe})_2\text{-1 b}]^{2-}$  indicates an antiaromatic character for the complex. Furthermore, this NICS(0) value was larger than that of the free-base form  $[\text{1 b}]^{2-}$  (4), indicating that the antiaromaticity of  $[\text{Sn}(\text{OMe})_2\text{-1 b}]^{2-}$  was stronger than that of  $[\text{1 b}]^{2-}$ . This result is consistent with the NMR measurements.

The mean plane deviation (MPD) values of the geometry-optimized structures of  $[\text{Sn}(\text{OMe})_2\text{-1b}]^{2-}$  and  $[\text{1b}]^{2-}$  were 0.177 Å and 0.471 Å, respectively (Figure S7). The significant difference in planarity suggests that coordination of the Sn(IV) ion likely enhances the planarity of isophlorin, which, in turn, leads to the observed increase in antiaromaticity. Notably, while the geometry-optimized structure of  $[\text{Sn}(\text{OMe})_2\text{-1b}]^{2-}$  closely matches its crystal structure,  $[\text{1b}]^{2-}$  exhibits relatively high planarity in the crystal. This discrepancy between the calculated and crystal structures of  $[\text{1b}]^{2-}$  may be attributed to crystal packing effects, which are not accounted for in the gas-phase calculations.

In the UV-Vis/NIR spectrum of **SnL<sub>2</sub>-1b** (Figure 7), two sharp absorption bands at approximately 450 and 600 nm and a broad weak band at 800–1200 nm are observed, which are similar to those of **[1a]<sup>2-</sup>**, and **[1c]<sup>2-</sup>** recorded under the same conditions.<sup>[12,13]</sup> This spectral similarity indicates that the two-electron reduction of **SnCl<sub>2</sub>-2b** occurs on the ligand rather than on the metal center. Time-dependent density functional theory

Table 2. NICS values for  $[\text{Sn}(\text{OMe})_3\text{-1b}]^{2-}$  and  $[\text{1b}]^{2-}$  [a]

Table 2. NICS values for $[\text{Sn}(\text{OMe})_2-1\text{b}]^{2-}$ and $[\text{1b}]^{2-}$ .			
	A	B	C
$[\text{Sn}(\text{OMe})_2-1\text{b}]^{2-}$	9 (50)	-6 (16)	0 (25)
$[\text{1b}]^{2-}$	4 (34)	-8 (2)	0 (24)

[a] NICS<sub>iso</sub> values are shown. NICS<sub>zz</sub> values are given in parentheses.

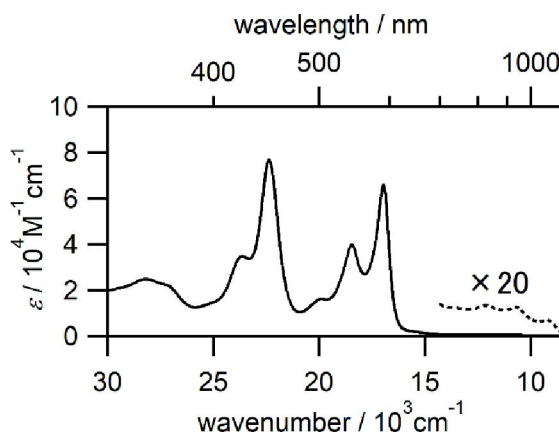


Figure 7. UV-Vis/NIR absorption spectrum of **SnL<sub>2</sub>-1b** in DMSO in the presence of NH<sub>2</sub>NH<sub>2</sub>·H<sub>2</sub>O (1%). The dashed line is magnified 20 times.

(TDDFT) calculations suggested that these absorption bands can be assigned to S<sub>0</sub>→S<sub>1</sub> (HOMO→LUMO), S<sub>0</sub>→S<sub>2</sub> (HOMO→LUMO+1), and S<sub>0</sub>→S<sub>3</sub> (HOMO-1→LUMO) transitions (Table S2 and Figure S9). For [1a]<sup>2-</sup>, and [1c]<sup>2-</sup>, weak absorption bands arising from the S<sub>0</sub>→S<sub>1</sub> (HOMO→LUMO) transition were observed around 1000 nm,<sup>[12,13]</sup> whereas **SnL<sub>2</sub>-1b** exhibited an absorption band that was more long-wavelength shifted, extending 1200 nm. This suggests that the HOMO-LUMO gap of **SnL<sub>2</sub>-1b** is smaller than those of [1a]<sup>2-</sup>, [1b]<sup>2-</sup>, and [1c]<sup>2-</sup>.

Similar to previously reported isophlorins [1a]<sup>2-</sup> and [1c]<sup>2-</sup>, **SnL<sub>2</sub>-1b** readily undergoes oxidation to form porphyrin **SnCl<sub>2</sub>-2b**. When attempting to extract **SnL<sub>2</sub>-1b** from a DMSO/diluted aqueous HCl solution with CHCl<sub>3</sub>, aerial oxidation occurred, converting **SnL<sub>2</sub>-1b** to **SnCl<sub>2</sub>-2b**. This was confirmed by <sup>1</sup>H NMR (Figure S5) and UV-vis/NIR (Figure S6) analyses, demonstrating the reversible nature of the interconversion between **SnL<sub>2</sub>-1b** and **SnCl<sub>2</sub>-2b**.

## Conclusions

We have synthesized and characterized the 20 $\pi$  antiaromatic Sn(IV)  $\beta$ -tetracyanoisophlorin complex **SnL<sub>2</sub>-1b**. The central Sn ion enhances the planarity of the isophlorin structure, resulting in stronger antiaromaticity compared to those of the free-base forms [1a]<sup>2-</sup> and [1c]<sup>2-</sup>. This enhanced antiaromaticity was confirmed by NMR spectroscopy, X-ray crystallography, and NICS calculations. Importantly, **SnL<sub>2</sub>-1b** is remarkably stable in air, in contrast to previously reported Si(IV) and Ge(IV) isophlorin complexes without cyano groups. This stability, combined with the ease of synthesis using mild reducing agents, makes **SnL<sub>2</sub>-1b** an attractive candidate for further studies and applications. The unique properties of **SnL<sub>2</sub>-1b**, including its tunable aromaticity/antiaromaticity and high stability, open new possibilities in catalysis and materials science. The ability to switch between the aromatic and antiaromatic states through redox processes may lead to the development of new molecular switches or sensors.

## Supporting Information Summary

The authors have cited additional references within the Supporting Information (Ref. [32–35]). Deposition Numbers 2385350 (for **SnCl<sub>2</sub>-2b**), 2385351 (for **[Sn(OMe)<sub>2</sub>-1b](PPh<sub>4</sub>)<sub>2</sub>**) contain the supplementary crystallographic data for this paper. These data are provided free of charge by the joint Cambridge Crystallographic Data Centre and Fachinformationszentrum Karlsruhe Access Structures service.

## Acknowledgements

This work was supported by JSPS KAKENHI Grant Number JP19H02688, Iketani Science and Technology Foundation (No. 0361035-A), and the Sasakawa Scientific Research Grant from The Japan Science Society (2023–3027). H. S. is grateful for a JSPS Research Fellow (24KJ1558). We thank Dr. Yosuke Tani (Osaka University) and Prof. Dr. Takuji Ogawa (Osaka University) for helpful discussion, and Mr. Laoviwat Pipatpong, (Mahidol University) for helping with the synthesis. The measurements were performed at the Analytical Instrument Facility, Graduate School of Science, Osaka University. The computation was performed using Research Center for Computational Science, Okazaki, Japan (Projects: 24-IMS-C238, 23-IMS-C224, and 22-IMS-C217).

## Conflict of Interests

The authors declare no conflict of interest.

## Data Availability Statement

The data that support the findings of this study are available in the supplementary material of this article.

**Keywords:** Antiaromaticity • Isophlorins • Porphyrinoids • Tin complexes • X-ray crystallography

- [1] B. K. Reddy, A. Basavarajappa, M. D. Ambhore, V. G. Anand, *Chem. Rev.* 2017, 117, 3420–3443.
- [2] P. Pushpanandan, M. Ravikanth, *Chem. Rec.* 2022, 22, e202200144.
- [3] R. B. Woodward, *Angew. Chem.* 1960, 72, 651–662.
- [4] J. A. Cissell, T. P. Vaid, A. L. Rheingold, *J. Am. Chem. Soc.* 2005, 127, 12212–12213.
- [5] J. A. Cissell, T. P. Vaid, G. P. A. Yap, *J. Am. Chem. Soc.* 2007, 129, 7841–7847.
- [6] A. Weiss, M. C. Hodgson, P. D. W. Boyd, W. Siebert, P. J. Brothers, *Chem. Eur. J.* 2007, 13, 5982–5993.
- [7] T. P. Vaid, *J. Am. Chem. Soc.* 2011, 133, 15838–15841.
- [8] R. Bachmann, F. Gerson, G. Gescheidt, E. Vogel, *J. Am. Chem. Soc.* 1992, 114, 10855–10860.
- [9] J. S. Reddy, V. G. Anand, *J. Am. Chem. Soc.* 2008, 130, 3718–3719.
- [10] S. P. Panchal, S. C. Gadekar, V. G. Anand, *Angew. Chem.* 2016, 128, 7928–7931.
- [11] S. P. Panchal, S. C. Gadekar, V. G. Anand, *Angew. Chem. Int. Ed.* 2016, 55, 7797–7800.
- [12] K. Yamashita, K. Nakajima, Y. Honda, T. Ogawa, *Chem. Eur. J.* 2020, 26, 3633–3640.

[13] H. Sugimura, K. Nakajima, K. Yamashita, T. Ogawa, *Eur. J. Org. Chem.* **2022**, e202200747.

[14] R. Cosmo, C. Kautz, K. Meerholz, J. Heinze, K. Müllen, *Angew. Chem. Int. Ed. Engl.* **1989**, *28*, 604–607.

[15] D. P. Arnold, J. Blok, *Coord. Chem. Rev.* **2004**, *248*, 299–319.

[16] B. Babu, J. Mack, T. Nyokong, *Dalton Trans.* **2023**, *52*, 5000–5018.

[17] J. H. Furhop, K. M. Kadish, D. G. Davis, *J. Am. Chem. Soc.* **1973**, *95*, 5140–5147.

[18] P. Cocolios, K. M. Kadish, *Isr. J. Chem.* **1985**, *25*, 138–147.

[19] K. M. Kadish, B. Boisselier-Cocolios, B. Simonet, D. Chang, H. Ledon, P. Cocolios, *Inorg. Chem.* **1985**, *24*, 2148–2156.

[20] R. Kumar, N. Chaudhri, M. Sankar, *Dalton Trans.* **2015**, *44*, 9149–9157.

[21] A. Antoniuk-Pablant, Y. Terazono, B. J. Brennan, B. D. Sherman, J. D. Megiatto, G. W. Brudvig, A. L. Moore, T. A. Moore, D. Gust, *J. Mater. Chem. A* **2016**, *4*, 2976–2985.

[22] N. Grover, M. Sankar, Y. Song, K. M. Kadish, *Inorg. Chem.* **2016**, *55*, 584–597.

[23] X. Ke, P. Yadav, L. Cong, R. Kumar, M. Sankar, K. M. Kadish, *Inorg. Chem.* **2017**, *56*, 8527–8537.

[24] X. Ke, R. Kumar, M. Sankar, K. M. Kadish, *Inorg. Chem.* **2018**, *57*, 1490–1503.

[25] M. R. Maurya, V. Prakash, T. A. Dar, M. Sankar, *ACS Omega* **2023**, *8*, 6391–6401.

[26] P. Rothemund, A. R. Menotti, *J. Am. Chem. Soc.* **1948**, *70*, 1808–1812.

[27] D. M. Collins, W. R. Scheidt, J. L. Hoard, *J. Am. Chem. Soc.* **1972**, *94*, 6689–6696.

[28] D. L. Cullen, E. F. Meyer Jnr, *Acta Crystallogr. B* **1973**, *29*, 2507–2515.

[29] D. P. Arnold, *Polyhedron* **1986**, *5*, 1957–1963.

[30] S. J. Webb, J. K. Sanders, *Inorg. Chem.* **2000**, *39*, 5920–5929.

[31] J. M. Barbe, C. Ratti, P. Richard, C. Lecomte, R. Gerardin, R. Guillard, *Inorg. Chem.* **1990**, *29*, 4126–4130.

[32] G. M. Sheldrick, *Acta Crystallogr. A* **2008**, *64*, 112–122.

[33] G. M. Sheldrick, *Acta Crystallogr. A Found. Adv.* **2015**, *71*, 3–8.

[34] M. J. Frisch, G. W. Trucks, H. B. Schlegel, G. E. Scuseria, M. A. Robb, J. R. Cheeseman, G. Scalmani, V. Barone, G. A. Petersson, H. Nakatsuji, X. Li, M. Caricato, A. V. Marenich, J. Bloino, B. G. Janesko, R. Gomperts, B. Mennucci, H. P. Hratchian, J. V. Ortiz, A. F. Izmaylov, J. L. Sonnenberg, D. Williams-Young, F. Ding, F. Lipparini, F. Egidi, J. Goings, B. Peng, A. Petrone, T. Henderson, D. Ranasinghe, V. G. Zakrzewski, J. Gao, N. Rega, G. Zheng, W. Liang, M. Hada, M. Ehara, K. Toyota, R. Fukuda, J. Hasegawa, M. Ishida, T. Nakajima, Y. Honda, O. Kitao, H. Nakai, T. Vreven, K. Throssell, J. A. Montgomery, J. E. Peralta, F. Ogliaro, M. J. Bearpark, J. J. Heyd, E. N. Brothers, K. N. Kudin, V. N. Staroverov, T. A. Keith, R. Kobayashi, J. Normand, K. Raghuvaran, A. P. Rendell, J. C. Burant, S. S. Iyengar, J. Tomasi, M. Cossi, J. M. Millam, M. Klene, C. Adamo, R. Cammi, J. W. Ochterski, R. L. Martin, K. Morokuma, O. Farkas, J. B. Foresman, D. J. Fox, Gaussian16, Revision C.01, Gaussian Inc., Wallingford, CT, 2016.

[35] M. Dolg, U. Wedig, H. Stoll, H. Preuss, *J. Chem. Phys.* **1987**, *86*, 866–872.

Manuscript received: September 30, 2024

Revised manuscript received: November 20, 2024

Accepted manuscript online: November 20, 2024

Version of record online: ■■■, ■■■

## RESEARCH ARTICLE



The synthesis and characterization of a novel air-stable Sn(IV)  $\beta$ -tetracyanoisophlorin complex is described. The complex was obtained by reducing the corresponding Sn(IV)  $\beta$ -tetracyanoporphyrin with hydrazine. NMR

spectroscopy and nucleus-independent chemical shift calculations confirmed increased antiaromaticity compared to the free-base analogs. The UV-Vis/NIR absorption spectrum was extended to 1200 nm.

H. Sugimura, K. Nakajima, K.-i.  
Yamashita\*

1 – 7

**Synthesis and Characterization of an Air-Stable Tin(IV)  $\beta$ -Tetracyanoisophlorin Complex: Enhanced Antiaromaticity through Metal Complexation**

